NANOSYSTEMS: PHYSICS, CHEMISTRY, MATHEMATICS, 2014, 5 (3), P. 343–353

CHANNELS OF ELECTRON-ELECTRON INTERACTIONS IN HIGHLY DOPED HETEROJUNCTION

V. A. Ambartsumyan[1], E. A. Andryushchenko[1], K. V. Bukhenskyy[1], A. B. Dubois[1], E. A. Dvoretskova[1], T. V. Gordova[2], N. I. Ivanova[3], S. I. Kucheryavyy[4], S. N. Mashnina[2], A. S. Safoshkin[1]

[1] Ryazan State Radioengineering University, Ryazan, Russia

[2] Moscow State University of Economics, Statistics and Informatics (Ryazan filial), Russia

[3] Moscow State University of Economics, Statistics and Informatics (Yaroslavl filial), Russia

[4] Institute of Atomic Energy of National Research Nuclear University of Moscow Engineer-Physics University, Obninsk, Russia

dubois.a.b@rsreu.ru

PACS 72.10.-d, 73.23.-b

Electron-electron interactions in a single highly doped heterojunction are considered, taking into account both intra- and intersubband transitions. Expressions are derived for the time of electron-electron interaction, matrix elements of the full screening potential and dynamic dielectric function in a 2D electron system with the fine structure of the energy spectrum, and for the electron density spatial distribution. The theoretical dependences $\tau_{ee}^{th}(T, n_s)$ provide a good description of the experimental times of Landau levels collisional broadening $\tau_q^{\exp}(T,\ n_s)$.

Keywords: electron-electron interactions, random phase approximation, Fourier analysis, Shubnikov-de Haas oscillations.

Received: 3 May 2014
Revised: 4 June 2014

1. Introduction

Starting from the pioneering works [1] and up to the present time [2-20], electron-electron (e-e) interactions are the subject of ever growing interest because of their fundamental role in kinetic phenomena. Among others, one should note the hot electrons effects, quantum corrections to the conductivity, and damping (destruction) of Landau qunatization in bulk and two-dimensional semiconductors with degenerate electrons. Also known are anomalies in the low-temperature magnetotransport arising when 2D electrons fill several size- quantized subbands. In particular, the authors of [2] predicted non-monotonous behavior of kinetic coefficients as the density of the 2D electrons is changed and several size-quantized subbands in a 2D system are filled. Experimentally, the reduction of mobility with the growth of electron surface density n_s was discovered in [3, 4]. Later [5 - 7], a complicated set of phenomena was discovered and studied in the $Al_xGa_{1-x}As/GaAs$ heterostructure whose potential well contained two size-quantized (the main E_m, and the first excited E_p) subbands. Most interesting among them are the amplitude and the frequency modulation of the transverse Shubnikov-de Haas (SdH) magnetoresistance [8], sharp bends in the magnetic field dependence of the oscillation amplitude $\delta(1/B)$ [9, 10] as well as the non-monotonous behavior of the Dingle temperature T_D with the 2D electron density n_s and

the temperature T [11, 12]. In spite of the variety of experimental details and approaches to their interpretation, the indicated effects were all shown to be caused by filling of the second excited size-quantized subband. The mechanism triggering the non-linear effects is the intersubband interaction. In [4, 5] following point was discussed; when the doping level of the $Al_xGa_{1-x}As\,(Si)\,/GaAs$ heterojunction is high enough for n_s to reach $8 \cdot 10^{11} cm^{-2}$, the quantum well contains two size-quantized subbands with energies E_m and E_p electron densities n_m and n_p, respectively, and the SdH oscillations of ρ_{xx} exhibit frequencies $F_{m,p} = (\pi h/e)\, n_{m,p}$ with the periods $\Delta_{m,p}\,(1/B) = F_{m,p}^{-1}$. The main feature is the modulation of the main frequency F_m amplitude with the frequencyF_p, the modulation depth growing with temperature and being more pronounced at the lower magnetic fields. The second feature is the development of oscillations at a different frequency $F_m - F_p$. These oscillations do not depend on temperature and transform to oscillations with a frequency F_m as the magnetic field is raised.

Assuming constant electron density and Fermi energy oscillations, Kadushkin [9, 10] explained the main features of the amplitude-frequency modulation of the SdH oscillations by the intersubband interaction. Authors of [2] derived an analytic expression for the amplitude of oscillations containing components at the frequencies $F_{m,p}$, $F_m - F_p$. They analyzed the experiments, taking into account the electron-phonon interaction. Formally, the Dingle temperature is related to the non- thermal collisional broadening time τ_q through the expression $T_D = \hbar/2\pi k\tau_q$. Description of the SdH oscillations of ρ_{xx} [8] based on the two subbands (m and p) model is in good agreement with the experimental results obtained in [12].

In the present paper, we report results from the study of e-e relaxation processes in a system of highly degenerate 2D electrons with finely structured energy spectrum and electron density spatial distribution. Expressions for the electron-electron intra-(τ_{ee}^{intra}) and intersubband (τ_{ee}^{inter}) interaction are derived and the matrix elements of the full screening potential $V_{tot}\,(q,\omega)$ and the dielectric function for $\chi\,(q,\omega)$ in the approximation far from the long wave limit are calculated. The oscillations in $\tau_q^{\exp}\,(T,n_s) \simeq \tau_{ee}^{th}\,(T,n_s)$ are shown to be related to the excitation of plasmons in the components of 2D electron system and the plasmon spectrum is studied.

2. Mechanism of Landau quantization destruction

One of the important points in the derivation of expressions for τ_{ee}^{intra} and τ_{ee}^{inter} is the calculation of the full screening potential matrix elements which, within the perturbation theory approach, implies the transformation of the potential $V\,(r,t)$ into $V_{tot}\,(q,\omega)$. In our problem, this corresponds to the following physical situation.

Let us consider 2D electrons, crystal lattice, and the source of perturbation as a thermodynamic system in equilibrium at the thermal bath temperature T. The electrons interact amongst themselves and with the crystal lattice with relaxation times τ_{ee} and τ_{eph}, respectively. At lower temperatures and in a quantizing magnetic field B, the equilibrium energy and momentum distribution of 2D electrons is given by harmonic oscillators with the cyclotron frequency ω_c. The electron states are correlated and coherent because of the strong e-e interaction with the relaxation times hierarchy $\tau_{ee} \ll \tau_p \ll \tau_\varepsilon$ where τ_p and τ_ε are the relaxation times of momentum p and energy ε. The electron states on the cyclotron orbits are coherent because the lifetime on these orbits exceeds the mean free time (momentum relaxation time). Although the electron state initial phase is determined by the electron settling into the cyclotron orbit and has a random nature, the motion of electrons on cyclotron orbits is synchronized and it is precisely this point that allows one to apply the random phase approximation (RPA) to these magnetized electrons. It is worthwhile to note

that the reduced Wigner radius for the studied heterojunctions with $n_s \simeq (0.5 \div 2) \cdot 10^{12} cm^{-2}$, $V(q, \omega)$ is $0.6 \div 1.2$, so that the use of RPA is rather justified [1].

Electron collisions with the crystal lattice defects destroy the ground quantum state (cyclotron orbits), which is seen in the broadening of Landau levels, resulting in finite values for the kinetic coefficients' oscillation amplitudes.

In the absence of an external electric field, the equilibrium state of electrons is characterized by the temperature T_D^0 which stipuleted the chaotization of the 2D electrons, which are in thermodynamic equilibrium with the crystal lattice (T, T_D^0) in the quantizing magnetic field B. Note that the perturbations of the potential relief of the quantum well's 2D channel, caused by various defects, are time-independent: $V(r, t)$. The electron system state (T, T_D^0) stationary with respect to the electron-lattice interaction is controlled through the energy and momentum relaxation with the characteristic time $\tau_{eph}^{(\varepsilon,p)}$.

The mechanism for the destruction of the quantum Landau state $(T, T_D^0)_B$ and development of a new equilibrium stationary state (T, T_D^*), which is not in equilibrium with respect to the initial equilibrium state (T, T_D^0), can be described in the following way. The electric field E causes a drift of the 2D electron system along the heterojunction quantum well (in the xy-plane) so that the electrons "scan" the spatial distribution of the heterojunction defects. In the reference frame associated with the 2D electrons, the observer sees the results of scanning the potential well defects as $V_{tot}(q, \omega)$. Here, the electric field E acts only as the means of sweeping the external (with respect to 2D electrons) perturbations, converting them into a time-dependent potential which is expressed in the transition from $V(r, t)$ to the Fourier component $V_{tot}(q, \omega)$.

In the 2D electron system perturbed by (T, T_D^0) the collisions acquire a different nature and at $T = const$ and $B = const$, the equilibrium broadening kT_D^0 is affected by the perturbation caused by the external field E so that a new equilibrium state with the broadening kT_D^0 is established. This new equilibrium state (T, T_D^*), should be considered as a non-equilibrium one with respect to $(T, T_D^0)_B$.

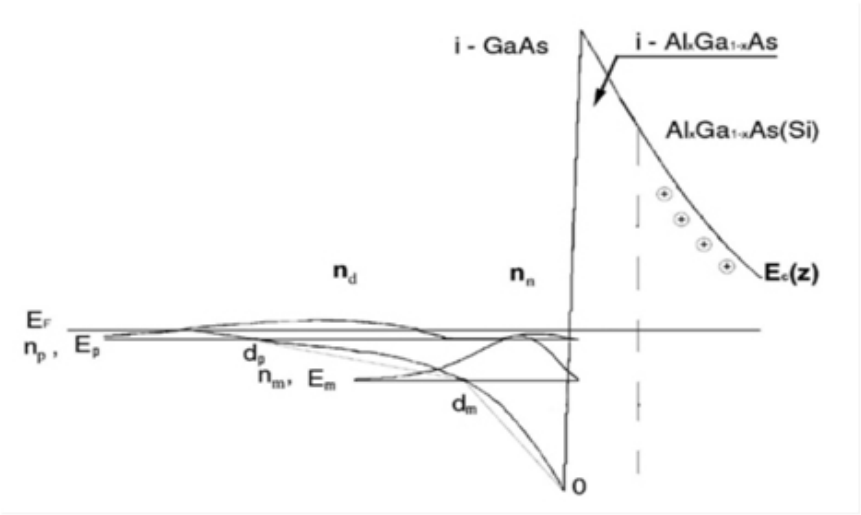

FIG. 1. The energy diagram of the conduction band $E_c(z)$ for a heterojunction with two filled size-quantized subbands E_m and E_p with electron densities n_m and $n_p = n_n + n_d$; d_p is the undoped spacer thickness, and $N_D^+, N_A^-, \Delta, \Lambda, \delta x$ are the sources of perturbation of the 2D electron system

Our analysis of e-e interaction is based on the calculation of the conduction band energy structure $E_c(z)$. We approximate the potential well of the heterojunction by a triangular profile [11] with the sharp bends at the size-quantized levels $E_m = E_c(d_m)$ and $E_p = E_c(d_p)$.

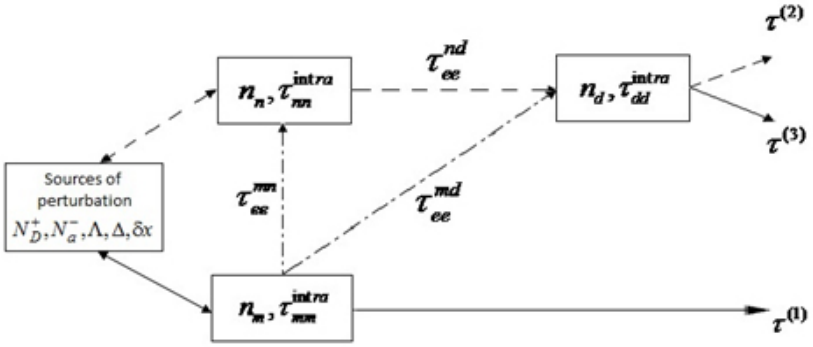

FIG. 2. Schematic model illustrating the channels through which the perturbation from the sources causing non-thermal collisional broadening of Landau levels passes. See text for details

Schematics of the e-e interactions in the 2D system is presented in Fig. 1, which also shows the typical channels through which the perturbation due to various sources, such as ionized donors N_D^+, acceptors N_a^-, growth islands of length Λ and height Δ, as well as the mole fraction variations δx, affects the electron system. Here, n_m, is the 2D electron density in the ground (main) size-quantized subband while n_n and n_d are the satellites of the perturbed (excited) subband component $n_p = n_n + n_d$ located close to ("near") and far from ("distant") the heterointerface (in the following referred to as the $n-$ and $d-$satellites). Of all the channels of Landau quantization damping which we consider, one should emphasize those three that reveal the major features. Since $n_m >> n_n, n_m$, and the centers of gravity of $|\psi(z)|^2$ at the levels E_m and E_p, are spatially resolved, the perturbation is sensed (absorbed) during time $\tau^{(1)}$ by the set of 2D electrons. Then, through the intrasubband (τ_{ee}^{mm}) and intersubband $(\tau_{ee}^{mn}, \tau_{ee}^{md}, \tau_{ee}^{nd})$ e-e interactions mediated by the (τ_{ee}^{nn}) and (τ_{ee}^{dd}) intrasubband interactions, the perturbation is extended to the entire 2D system. The path of this mechanism is shown in Fig.1 by the solid line:

$$\tau^{(1)} \Rightarrow (\tau_{ee}^{mn}) \Rightarrow \left(\tau_{ee}^{nd}, \tau_{ee}^{mn}\right) \Rightarrow \left(\tau_{ee}^{nn}, \tau_{ee}^{dd}, \tau_{ee}^{nd}\right) = \tau_{ee}^{(1)}. \quad (1)$$

The major factor here is the interaction of n_m, and n_d electrons $(m-d)$, while n_n, is a passive element. The second scenario corresponds to the situation where perturbation is first sensed by the $n-$satellite. In that case, the time needed to destroy the quantization is formed in the chain shown in Fig.1 by the dashed line:

$$\tau^{(2)} \Rightarrow (\tau_{ee}^{nn}) \Rightarrow \left(\tau_{ee}^{nd}\right) \Rightarrow \left(\tau_{ee}^{mn}, \tau_{ee}^{nd}\right) \Rightarrow \left(\tau_{ee}^{nn}, \tau_{ee}^{dd}, \tau_{ee}^{nd}\right) = \tau_{ee}^{(2)}. \quad (2)$$

Here, the system behavior is governed by the intersubband $''n-d''$, $''n-m''$ and $''m-d''$ interactions. The $''n-d''$- interaction is the major one in this channel and n_m, plays the role of a passive element. The third version is formed in the chain where the $''m-n''$ interaction dominates while n_d is a passive element:

$$\tau^{(3)} \Rightarrow (\tau_{ee}^{mm}) \Rightarrow \left(\tau_{ee}^{mn}, \tau_{ee}^{md}\right) \Rightarrow \left(\tau_{ee}^{nn}, \tau_{ee}^{dd}, \tau_{ee}^{nd}\right) = \tau_{ee}^{(3)}. \quad (3)$$

The corresponding path is shown by the dot-and-dash line. With respect to the nature of induced transitions the e-e interactions can be classified into three types: (1) interactions within a single subband limited to the transitions within the same subband; (2) intrasubband interaction exciting the intersubband transitions, and (3) intersubband interactions also resulting in intrasubband transitions.

To within the second order in the external potential $V_{tot}(q,\ \omega)$ in the perturbation theory expansion, the time required for the e-e interaction to change the state $\langle k|\, p\rangle$ into $\langle k+q|\, p-q\rangle$ is given by a well-known expression:

$$\frac{1}{\tau_{ij}^{ee}} = \int\limits_{-\infty}^{\infty} d\omega \sum_{k,m}\sum_{q} \left|V_{tot}^{ijkl}(q,\omega)\right|^2 \times \\ \times \sum_{k,p} \delta\left(E_j(k+q) + E_l(p-q) - E(k) - E_k(p)\right) f_k f_p (1-f_{k+q})(1-f_{p-q}), \quad (4)$$

where indices i, j, k, l run over the set consisting of symbols m (main component) and n, d (satellites of the n_p-component) which label the electron transition type; f - Fermi-Dirac function. Using the notations given in [12 - 20], (4) can be written as:

$$\frac{1}{\tau_{ij}^{ee}} = \int\limits_{-\infty}^{\infty} \frac{d\omega}{\pi^2 \mathrm{ch}^2(\hbar\omega/2k_BT)} \sum_{k,m}\sum_{q} \left|V_{tot}^{ijkl}(q,\omega)\right|^2 \chi_{ik}(q,\omega)\,\chi_{jk}^{*}(q,\omega). \quad (5)$$

Matrix elements of the $m-n$, $m-d$ intersubband interactions were calculated with the wave functions $\psi_m(z)$ as well as the $\psi_n(z)$ and $\psi_d(z)$ components of the wave function $\psi_p(z)$ with appropriate boundary conditions.

Taking into account the parameters of the energy band diagram, the matrix elements of the full screening potential for the first and second type transitions are reduced to the form:

$$V_{tot}^{ijkl}(q,\omega) = \frac{E_j}{2d_l S\left(q^3 + 2\pi e^2 q^3 \chi_{ik}(q,\omega)\right)}, \quad (6)$$

where $S = L^2$ - square of 2D system.

For $i = k$ and $j = l$, while for the third type:

$$V_{tot}^{ijkl}(q,\omega) = \frac{E_j(1-qd_j) - E_j(1+qd_i)}{2(d_i-d_j)S\left(q^3 + 2\pi e^2 q^4 \chi_{ik}(q,\omega)\right)}, \quad (7)$$

with $i = j$ and $k = l$. In the form convenient for calculations, the relaxation times for the first and second type transitions are written as:

$$\frac{1}{\tau_{ij}^{intra}} = \frac{E_j^2 m^{*2} S}{16\pi^5 d_j^2 \hbar^4 n_i n_j} P_{-n}(T), \quad (8)$$

while for the third type:

$$\frac{1}{\tau_{li}^{inter}} = \frac{m^{*2} S}{8\pi^6 (d_i - d_m)^2 \hbar^4} \left\{ \frac{(E_i - E_m)^2}{8\pi} Q_{-n}(T) - \frac{(E_i - E_m)(E_l d_m + E_m d_i)}{\sqrt{8\pi}} W_{-n}(T) \right\} \quad (9)$$

for $i \neq l$. The polynomials in (8) and (9) are:

$$P_{-n}(T) = \frac{B_1}{T} + \frac{B_2}{T^2} + \frac{B_3}{T^3} + ...,$$

$$Q_{-n}(T) = \frac{B_1}{T} - \frac{B_2}{T^2} + \frac{B_3}{T^3} - ...,$$
$$W_{-n}(T) = \frac{B_2}{T^2} + \frac{B_4}{T^4} + ...$$

with the coefficients B_k defined by the Riernann zeta-function $\varsigma(z, v)$. The non-monotonous behavior of $\tau_{ee}^{-1}(T)$ is determined by the uniformly converging sums $P_{-n}(T)$, $Q_{-n}(T)$ and $W_{-n}(T)$ multiplied by the zeta- and gamma-functions [9]:

$$\varsigma(z, v) = \frac{1}{\Gamma(z)} \int_0^\infty \frac{t^{z-1} e^{-vt}}{1 - e^{-t}} dt,$$

where $z = \frac{d_m}{d_m + d_p}$; $v = \frac{\hbar^2 \pi}{2k_B T} \left(\frac{n_m n_p}{n_m + n_p} \right)^{\frac{1}{2}}$.

The products of $P_{-n}(T)$, $Q_{-n}(T)$ and $W_{-n}(T)$ with $\varsigma(z, v)$ are rather sensitive to the electron concentration in the size-quantized subbands. For example, for $n_m > 8 \cdot 10^{11} cm^{-2}$ ($n_d = 0.1 n_m$, $n_n = 0.1 n_d$, $d_p/d_m = 3.5$) the factor $\varsigma(z, v)$ in (9) results only in some smoothening of the non-monotonous behavior while at $n_m > 8 \cdot 10^{11} cm^{-2}$ the curve $\tau_{ee}^{-1}(T)$ does not contain any non-monotonous parts at all.

Calculations of τ_{ee}^{th} were performed within the outlined schematic model of the Landau quantization destruction, taking into account the paths corresponding to channels (1-3), including both intra- and intersubband transitions according to (8) and (9) employing the Matthiessen rule $\tau_{ee}^{-1} = \sum_i (\tau_{ee}^{-1})_i$, where the summation is performed over all intra- and intersubband components of the schematic model presented in Fig. 2.

3. Electron "bottleneck"

Presented for comparison in Figs. 3a and 3b are the experimentally measured and calculated curves $\tau_q^{\exp}(T, n_s)$ and $\tau_{ee}^{th}(T, n_s)$ for several heterostructure samples where 2D electrons are certainly known to fill only the lowest size- quantized subband ($n_s < 8 \cdot 10^{11} cm^{-2}$). Figures 4a and 4b show the experimental and calculated curves for the time of destruction of Landau quantization for two heterostructures with electron density sufficient for filling of the two size-quantized subbands (see [9, 10] for the details of the analysis of the experiment).

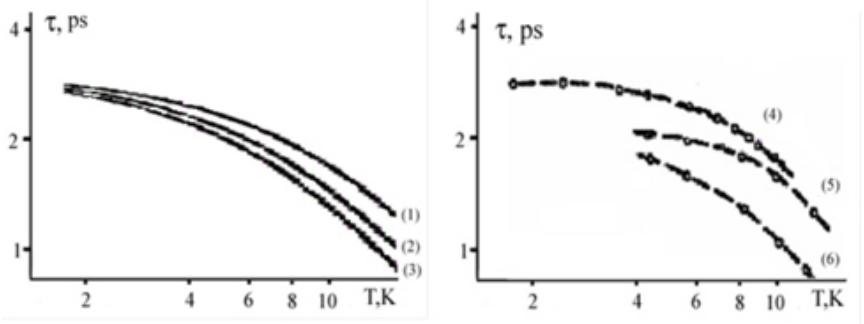

FIG. 3. Comparison of the experimental $\tau_q^{\exp}(T)$ (n_m,n_d or n_n) [2] (a) and calculated $\tau_{ee}^{th}(T)$ (b) curves for different values of the $m-$subband electron density: $n_m, 10^{11} cm^{-2}$: $1, 4 - 8.5$; $2, 5 - 6.9$; $3, 6 - 6.3$

The energy and geometrical parameters were taken from the energy diagrams $E(z)$ for the samples with appropriate electron densities. The first result is a quantitative "hit" of

the calculated times into the range of T in the studied temperature interval $2 \leqslant T \leqslant 12K$ for the real densities $n_m \approx 10^{12} cm^{-2}$, $n_d = 0.1 n_m$, $n_n = 0.01 n_m$ and, respectively, $d_p/d_m = 3$. Of all the considered versions of the model presented in Fig.2, scenario (3) is the most satisfactory one and the curve $\tau_{ee}^{th}(T, n_s)$, plotted in Fig. 4b, was calculated exactly for this scenario. Further, it should be noted that at low temperatures ($T < 5K$), the Landau quantization damping is governed by n_m-electrons. Numerical analysis of the expansion of the dielectric functions (6) reveals the appearance of non- monotonous parts in the curve $\tau_{ee}^{th}(T, n_s)$ at $n_m > 8 \cdot 10^{11} cm^{-2}$ and $T > 5K$ (see (10-13)), allowing one to argue [9,10] that the typical oscillations of $\tau_{ee}^{th}(T)$ arise only after the electrons fill the second excited size-quantized subband and for the system response to the thermal perturbation at $T > 5K$. The third obtained result is the role of n_n-satellite in the appearance of the oscillations regardless of which component of the 2D electron system senses the perturbation, as shown in Fig.2 by channel $\tau^{(3)}$.

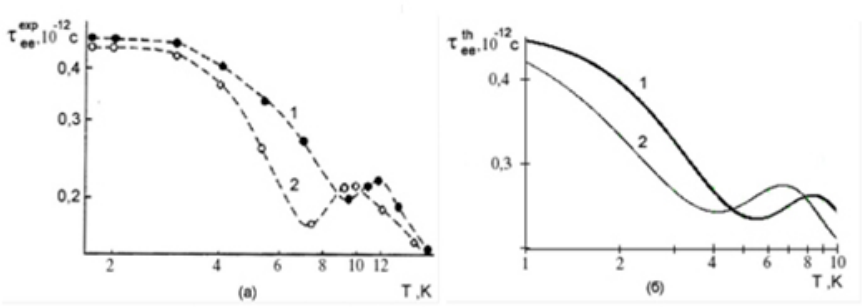

FIG. 4. Comparison of the experimental $\tau_q^{\exp}(T)$ [2] (a) and calculated $\tau_{ee}^{th}(T)$ (b) curves for different values of the $m-$subband electron density: $1 - 9.1$; $2 - 10.0$

This was also directly seen in (9). Indeed, for $n_n = 0$, only $\tau_{mm}^{intra}(T)$ and $\tau_{dd}^{intra}(T)$ are different from zero and no oscillations arise in $\tau_{ee}^{th}(T)$. The bottleneck effect is explained in the following way; variation of temperature initiates the frequency scan of the external perturbation $V_{tot}(q, \omega)$ towards higher ω. The 2D electron system is transparent for $V_{tot}(q, \omega)$ until the frequency ω_τ of one of the components (n_m n_d, or n_n) is reached. The lowest ω_τ corresponds to the n_n-satellite and it is this component or, to be more precise, its intrasubband relaxation that is the bottleneck for $V_{tot}(q, \omega)$, perturbing the 2D electron system as a whole and finally destroying the cyclotron orbit quantization (damping of Landau quantization). This bottleneck effect in the e-e interactions illustrates the coincidence of the resonant frequencies for $''m - n''$and $''d - n''$ channels (see Fig. 5 (curves 1 and 3) below in the range of low frequencies).

Thus, the experimentally observed features in $\tau_q^{\exp}(T)$ at $T < 5K$ are only related to the intrasubband e-e transitions, $\tau_q^{\exp}(T) \approx \tau_{ee}^{th}(T) \approx \tau_{mm}^{intra}(T)$. At higher temperatures, a mixed mechanism of the Landau quantization destruction is realized:

$$\tau_q^{\exp} \approx \tau_{ee}^3 \left[(\tau_{ee}^{mn})^{-1} = \left(\tau_{mn}^{\text{int}\,ra}\right)^{-1} + \left(\tau_{mn}^{\text{int}\,er}\right)^{-1}; \left(\tau_{ee}^{nd}\right)^{-1} = \left(\tau_{nn}^{\text{int}\,ra}\right)^{-1} + \left(\tau_{nd}^{\text{int}\,er}\right)^{-1} \right].$$

It should be noted that by varying the well parameters, one can obtain a satisfactory agreement with experimental results. This technique offers the possibility of recovering the actual potential profile from the superposition of the curves $\tau_q^{\exp}$ and τ_{ee}^{th}, measured for the

samples with different doping levels, and therefore, showing different variations of the form-factors d_p/d_m and E_p/E_m. However, this matching of the calculated curves τ_{ee}^{th} with the experimental ones $\tau_q^{\exp}$ is limited by a certain arbitrariness in the adjustable parameters d_p/d_m and E_p/E_m (the potential well form-factors) since the curve $E(z)$ cannot be derived with sufficient accuracy because of the uncertainties in N_D, N_A and the band discontinuity $\Delta E_c/\Delta E_g$ for the AlGaAs/GaAs heterostructure [7, 9, 10].

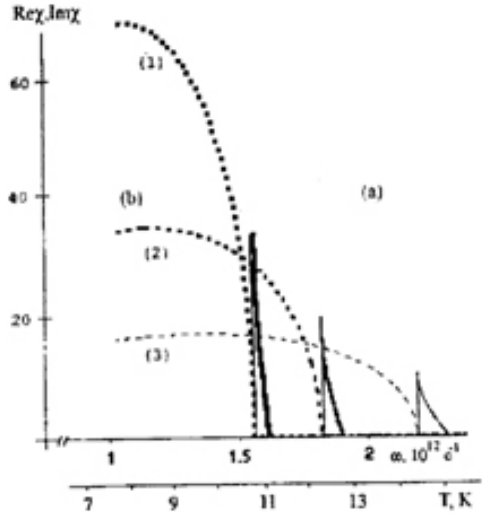

FIG. 5. Frequency dependence of the dielectric function for the interaction between the main size-quantized $m-$subband electrons with the $n-$satellite of the $p-$subband. $n_m, 10^{11} cm^{-2}$: $(1) - 8.5, (2) - 10, (3) - 11.5$; $d_p/d_m = 3.5$

4. Spectrum of collective excitation

Bearing in mind the oscillations in $\tau_q^{\exp}$ and τ_{ee}^{th}, it is natural to expect the resonant response of the components of a complex 2D electron system to the external perturbation $V_{tot}(q,\omega)$ at the plasma oscillations' frequency. The 2D system responds to the spectrum of $V_{tot}(q,\omega)$ by one of its n_m, n_n, n_d components (or their combination), and in a time$\tau_{ee}(\tau_{ee}^{intra}, \tau_{ee}^{inter})$, the perturbation extends to the entire system resulting in the destruction of quantum states (cyclotron orbits), which is experimentally observed as the reduction of the $\delta(1/B)_T$ oscillations' amplitude. The latter is formally equivalent to the rise of temperature T at which the measurements are taken. Therefore, the resonant response featuring the Landau quantization destruction corresponds to a minimum in the curves $\tau_q^{\exp}$ and τ_{ee}^{th}. We have performed a spectral analysis of the dispersion equations (6) for $\chi(q,\omega)$ for various channels of e-e interactions according to the scheme shown in Fig. 2 and various relative values of the densities n_m, n_n, n_d in the situation where two size-quantized subbands are occupied ($n_m > 8 \cdot 10^{11} cm^{-2}$). The plasma oscillation frequencies ω_τ are found from the dispersion equation $\chi(q,\omega) = 0$, the minima in $\tau_{ee}^{th}(T)$ corresponding to the minima in $\operatorname{Re}\chi(q,\omega)$ and $\operatorname{Im}\chi(q,\omega) = 0$ while the maxima in $\tau_{ee}^{th}(T)$ correspond to $\operatorname{Re}\chi(q,\omega) = 0$ and maxima in $\operatorname{Im}\chi(q,\omega)$ [1, 19].

To calculate $\operatorname{Re}\chi(q,\omega)$ and $\operatorname{Im}\chi(q,\omega)$, the expression (6) should be take in the form of function $\chi(\omega)$:

$$\chi_{ik}(\omega) = \frac{1}{S}\sum_q \chi_{ik}(q,\omega). \tag{10}$$

Taking into account the characteristic scales $q \in \left\{d_m^{-1}, d_p^{-1}\right\}$ of the 2D electron system, the summation over q results in the expression:

$$\chi_{ik}(\omega) = f(n_i, \omega) + f(n_k, \omega), \tag{11}$$

where

$$f_i(n_i,\omega) = L\sqrt{n_i}\left\{\frac{1}{L\sqrt{n_i}} - \left[\sqrt{2\pi} - \left(\frac{m^*\omega L}{\hbar\sqrt{n_i}\pi} - \sum_{k=1}^{\infty}\left\{\frac{(-1)^{k-1}}{2k(2k)!}\left(\frac{m^*\omega L}{\hbar\sqrt{n_i}\pi}\right)^{2k}\right\}\right)^2\right]^{1/2} - \right.$$
$$\left. - \left[\sqrt{2\pi} - \left(\frac{m^*\omega L}{\hbar\sqrt{n_i}\pi} - \sum_{k=1}^{\infty}\left\{\frac{(-1)^{k-1}}{2k(2k)!}\left(\frac{m^*\omega L}{\hbar\sqrt{n_i}\pi}\right)^{2k}\right\}\right)^2\right]^{1/2}\right\}. \tag{12}$$

The latter expression reduces to:

$$f_i(n_i,\omega) = L\sqrt{n_i}\left\{\frac{1}{L\sqrt{n_i}} - \left[\sqrt{2\pi} - \left(\frac{m^*\omega L}{\hbar\sqrt{n_i}\pi} - \ln\left(\frac{m^*\omega L}{\hbar\sqrt{n_i}\pi}\right) + C - \mathrm{Ci}\left(\frac{m^*\omega L}{\hbar\sqrt{n_i}\pi}\right)\right)^2\right]^{1/2} - \right.$$
$$\left. - \left[\sqrt{2\pi} - \left(\frac{m^*\omega L}{\hbar\sqrt{n_i}\pi} + \ln\left(\frac{m^*\omega L}{\hbar\sqrt{n_i}\pi}\right) - C + \mathrm{Ci}\left(\frac{m^*\omega L}{\hbar\sqrt{n_i}\pi}\right)\right)^2\right]^{1/2}\right\}, \tag{13}$$

where C is the Euler constant, $f(n_k, \omega)$ is given by (12) and (13) after the substitution of n_i by n_k; $\mathrm{Ci}(x) = \int\limits_{-\infty}^{x} \frac{\cos t}{t} dt$ - integral cosinus. The alternating sums over k in (12) prove to be rapidly converging. Fig. 5 illustrates the partial contributions of various mechanisms to the Landau quantization destruction and the density-dependent singularities. For example, plotted in Fig. 5 are the frequency dependences $\mathrm{Re}\,\chi(q,\omega)$ and $\mathrm{Im}\,\chi(q,\omega)$ for $n_m \approx 10^{12} cm^{-2}$ for three intersubband transition channels. It is seen that the $n_m - n_n$ and $n_n - n_d$ interactions are dominat. Moreover, the resonant frequency is determined by the $n-$satellite density. Shown in Fig. 5 is the influence of the second size-quantized subband filling factor. An increase in the density n_m, (and hence n_n and n_d) results in the resonant frequency shift to higher values while the discontinuity.in $\mathrm{Re}\,\chi(q,\omega)$ and $\mathrm{Im}\,\chi(q,\omega)$ is reduced which is consistent with the third scenario of the schematic model presented in Fig. 2 (domains "a" the real and "b" the imaginary parts of $\chi(\omega)$).

Similar analysis of the other channels for paths (1) and (2) of the model presented in Figs. 2 confirmed on the whole the trends presented in Fig. 5.

It should be noted here that in [12], the curve $\tau_{ee}(T)$ was obtained for a pair of coupled rectangular wells in the long wavelength limit at $T = 0$, which is incompatible with tile conditions of the experiments reported in [9]. In that case [12], the calculations of $\tau_{ee}(T)$ result in divergences which cannot be neglected when solving a particular problem. On the other hand, formulas of the type of (9) and (10) derived by us for the inter- and intrasubband e-e interactions allow one to obtain expressions for $\tau_{ee}^{intra}(T)$ and $\tau_{ee}^{inter}(T)$ given in [12] with the coefficients B_i in (8, 9) do not containing any divergencies.

5. Conclusions

In conclusion, it should be noted that a similar problem for 2D electrons seems to have been first considered in [12], and since then, numerous attempts have been undertaken [13-18] to study this problem for 2D electron system where several size-quantized subbands are filled at $T \neq 0$ in the long wavelength limit. However, the plasma oscillation spectrum has not been obtained in any of these works. Characteristic features of 2D electron systems, such as the amplitude-frequency modulation, beatings, and sharp bends in the oscillation amplitude magnetic field dependence make the description of Landau quantization damping, in terms of the Dingle temperature, rather problematic. Another point to be considered is the fact that in the magnetic field range where a strong amplitude-frequency modulation takes place, the $p-$subband electrons are in the state close to the quantum limit and one can only speak of the oscillation's period in a rather limited sense.

Acknowledgements

Authors thank Prof. Yu. E. Lozovik, L. A. Falkovskyy, G. S. Lukyanova and A. I. Novikov for fruitful discussions.

References

[1] Pines D., Nozieres P. *The theory of quantum liquids*. W.A. Benjamin, Inc. New York, Amsterdam, 383 p. (1966).
[2] Leadley D. R., Nicholas R. J., Harris J. J., Foxon C. T. Inter-subband scattering rates in GaAs–GaAlAs heterojunctions. *Sem. Sci. Tech*, **5**, P. 1081–1089 (1990).
[3] Lee S. C., Galbraith I. Intersubband and intrasubband electronic scattering rates in semiconductor quantum wells. *Phys. Rev. B.*, **59**(24), P. 15796–15805 (1999).
[4] Coleridge P. T. Intersubband scattering in a 2D electron gas. *Semicond. Scl. Technol.*, **5**, P. 961–968 (1990).
[5] Coleridge P. T. Small-angle scattering in two-dimensional electron gases. *Phys. Rev. B.*, **44**(8), P. 3793–3801 (1991).
[6] Itskovsky M. A., Maniv. T. Fourier analysis of the de Haas-van Alphen oscillations in two-dimensions electron systems with background reservoir states. *Phys. Rev. B.*, **64**(17), P. 174421/1-174421/7 (2001).
[7] Halvorsen E., Galperin Y., Chao K. A. Optical transitions in broken gap heterostructures. *Phys. Rev. B.*, **61**(24), P. 16743-16749 (2000).
[8] Averkiev N. S., Monakhov A. M., Sablina N. I., Koenraad P. M. On the experimental data processing of the magnetoresistance oscillationsin two-dimensional electron gas. *Semiconductors*, **37**(2), P. 169–172 (2003).
[9] Kadushkin V. I., Dubois A. B., Gorbunova Yu. N., Tsahhaev F. M. Plasma Oscillations in Q2D Electron System with the Fine Structure of Energy Spectrum. *Phys. Low-Dim. Struct.*, **5**(6), P. 107–132 (2004).
[10] Kadushkin V. I., Dubois A. B. Bottleneck in Electron Electron Interactions and Anomalies in the Landau Quantization Damping. *Phys. Low-Dim. Struct.*, **7**(8), P. 7–24 (2003).
[11] Dubois A. B., Zilotova M. A., Kucheryavyy S. I., Safoshkin A. S. Kinetic processes in moderately doped heterojunction. *Vestnik of RSREU*, **3**(45), P. 88–92 (2013).
[12] Slutzky M., Entin-Wohlman O., Berk Y., Palevsky A. Electron-electron scattering in coupled quantium wells. *Phys. Rev. B.*, **53**(7), P. 4065–4072 (1996).
[13] Hatke A. T., Zudov M. A., Pfeiffer L. N., West K. W. Role of electron–electron interactions in magnetoresistance oscillations in high-mobility 2D electron systems. *Physica E*, **42**, P. 1081–1083 (2010).
[14] Glazov S. Yu., Kubrakov E. S., and Meshcheryakova N. E. Plasma Oscillations in Two-Dimensional Electron Systems with a Superstructure under Stark Quantization Conditions. *Physics of Wave Phenomena*, **18**(4), P. 313–317 (2010).
[15] Hatke A. T., Zudov M. A., Pfeiffer L. N., West K. W. Role of electron-electron interactions in nonlinear transport in two-dimensional electron systems. *Phys. Rev. B.*, **79**(16), P. 161308(R) (2009).
[16] Raichev O. E. Magnetoresistance oscillations in two-subband electron systems: Influence of electron-phonon interaction. *Phys. Rev. B.*, **81**, P. 195301 (2010).

[17] Sica G., Polini M., Tosi M. P. Electron Electron Interactions In The 2D Ferromagnetic Electron Fluid. *Modern Physics Letters B*, **15**(24), P. 1053–1059 (2001).

[18] Goh K. E.J., Simmons M.Y., Hamilton A.R. Electron-electron interactions in highly disordered two-dimensional systems. *Phys. Rev. B.*, **77**, P. 235410 (2008).

[19] Dubois A. B. Electron-electron interactions in moderately-doped heterojunction. *Proceedings of Moscow Institute of Physics and Technology (State University)*, **2**, 1(5), P. 24–27 (2010).

[20] Dubois A. B. Plasma Oscillations and Electron–Elecron Interactions in 2D Electron Systems. *Journal of Physics: Conference series*, **129**, P. 012025 (2010).